ADVANCED HEALTHCARE MATERIALS

www.advhealthmat.de

A Multimaterial Microphysiological Platform Enabled by Rapid Casting of Elastic Microwires

Yimu Zhao, Erika Yan Wang, Locke Huyer Davenport, Yin Liao, Keith Yeager, Gordana Vunjak-Novakovic, Milica Radisic, and Boyang Zhang**

Due to escalating drug developmental costs and limitations of cardiotoxicity screening, there is an urgent need to develop robust in vitro 3D tissue culture platforms that can both facilitate the culture of human cardiac tissues and provide noninvasive functional readouts predictive of cardiotoxicity in clinical settings. However, such platforms commonly require complex fabrication procedures that are difficult to scale up to high-throughput testing platforms. Here, innovative multimaterial processing into a scalable and functional platform is proposed in the format of a 96-well plate. Three classes of materials are integrated into the platform. An array of soft elastic microwires is used both as anchors for tissue formation as well as sensors for recording tissue contraction. Conductive carbon electrodes are embedded into the plate to drive electrical stimulation for tissue maturation and pace tissue contraction during drug testing. The bulk of the device is made of rigid polystyrene plastic to eliminate drug-absorbing polydimethylsiloxane (PDMS). The platform has higher throughput than the current state-of-the-art devices, at a significantly reduced cost of manufacturing and tissue production.

1. Introduction

Cardiotoxicity is a major cause of drug failure at the later stages of clinical trials and it is linked to a number of postmarket withdrawals.[1,2] Validating the safety of candidate drugs and eliminating unqualified candidates as early as possible is key for reducing the costs of drug discovery and preventing patient fatality.[3] Although conventional monolayer cultures with immortalized cell lines enable high-throughput screening, they have limited relevance to native myocardium due to the lack of tissue level function and morphological organization.[4] Engineered cardiac tissues from human stem cell derived cardiomyocytes have been shown to more closely mimic the myofiber bundles of the native cardiac muscle, exhibiting an aligned sarcomere structure and remarkable levels of contractile forces.[5] However, manufacturing reproducible 3D tissues in large quantities requires complicated fabrication processes, which involve building hollow or suspended microstructures that are important to promote functional tissue formation.[6] Furthermore, detecting cardiotoxicity also requires functional readouts from engineered cardiac tissues.

Built-in sensors have been incorporated in many microphysiological platforms. For example, Shim et al. created thin muscle films on top of a thin layer of polydimethylsiloxane (PDMS) or a polyurethane film. Deformation of the films could be easily modeled and correlated to force of contraction generated by overlaid cardiomyocytes.[7] More recently, Lind et al. incorporated this method and embedded an electrical circuit in the thin polymer film using 3D printing.[8] This technology can translate electrical signal of an embedded resistor into contractile dynamics using modeling techniques. However, these systems only allow culture of cell monolayers of structures that are several cell layers thick. Widely used two-post platforms adopted PDMS posts as force sensors to noninvasively report force of contraction from a 3D tissue.[9,10] However, cultivated tissues are prone to slipping off from the posts resulting in device failure. In addition, these devices rely on the use of PDMS, which is prone to drug absorption due to its hydrophobic nature.[11]

We show here that tissue detachment can be prevented by omitting the two-post design, and focusing on a pair of

Y. Zhao, L. H. Davenport, Y. Liao, Dr. M. Radisic
Department of Chemical Engineering and Applied Chemistry
University of Toronto
Toronto, ON M5S 3E5, Canada
E-mail: m.radisic@utoronto.ca

E. Y. Wang, L. H. Davenport, Dr. M. Radisic, Dr. B. Zhang
Institute for Biomaterials and Biomedical Engineering
University of Toronto
Toronto, ON M5S 3G9, Canada
E-mail: by.zhang@utoronto.ca

Dr. K. Yeager, Dr. G. Vunjak-Novakovic
Laboratory for Stem Cells and Tissue Engineering
Department of Biomedical Engineering
Columbia University
New York, NY 10032, USA

Dr. G. Vunjak-Novakovic
Department of Medicine
Columbia University
New York, NY 10032-3784, USA

Dr. M. Radisic
Toronto General Research Institute
University Health Network
Toronto, ON M5G 2C4, Canada

Dr. M. Radisic
The Heart and Stroke/Richard Lewar Centre of Excellence
Toronto, ON M5S 3H2, Canada

DOI: 10.1002/adhm.201801187

suspended elastic microwires for tissue anchorage. Instead of PDMS, we use the hard plastics, such as polystyrene, that is widely used in biological research and drug screening in the pharmaceutical industry. However, the manufacturing and integration of suspended soft elastic microwires with rigid polystyrene structures in a scalable manner is a challenge from a material manufacturing standpoint.

To produce flexible features on a hard substrate, challenges lie in the conventional micromolding process requirement that the microfeatures and the bulk device to be made of a single material, as is the case often when post-devices are made out of PDMS. To overcome this challenge, we present a unique technique for rapidly casting of elastic suspended microstructures with conductive electrodes on hot-embossed hard polystyrene plates. These plates allow scalable production of cardiac microtissues in a 96-well plate format with built-in force sensors and electrodes. This manufacturing method allowed us to produce a device that integrates three materials with distinct properties: 1) elastic microwires for force sensing, 2) conductive carbon electrodes for long-term electrical stimulation, and finally 3) the bulk device made of hard inert polystyrene. The combination of force sensors and electrodes allowed us to noninvasively apply electrical inputs as well as extract functional readouts. The suspended polymer wires served as reliable anchor points as well as force sensors for the cardiac tissues. In the 96-well plate format, tissue size was reduced compared to our previous work, hence further reducing cell usage and cost.[6] The adoption of multiwell plate format is also an important step to move the field of organ-on-a-chip toward scalable production and experimentation.

2. Results

2.1. Device Description

Our tissue culture platform (referred to here as a Biowire II plate) was made of tissue culture plastic (polystyrene) yielding a PDMS-free final product, which minimizes drug absorption.[12] The platform is based on a footprint of a standard 96-well plate, giving compatibility with widely used plate readers. The device was assembled from four components: 1) plate cap, 2) bottomless 96-well plate, 3) polymer wire array, and 4) patterned polystyrene base (**Figure 1**). The plate cap

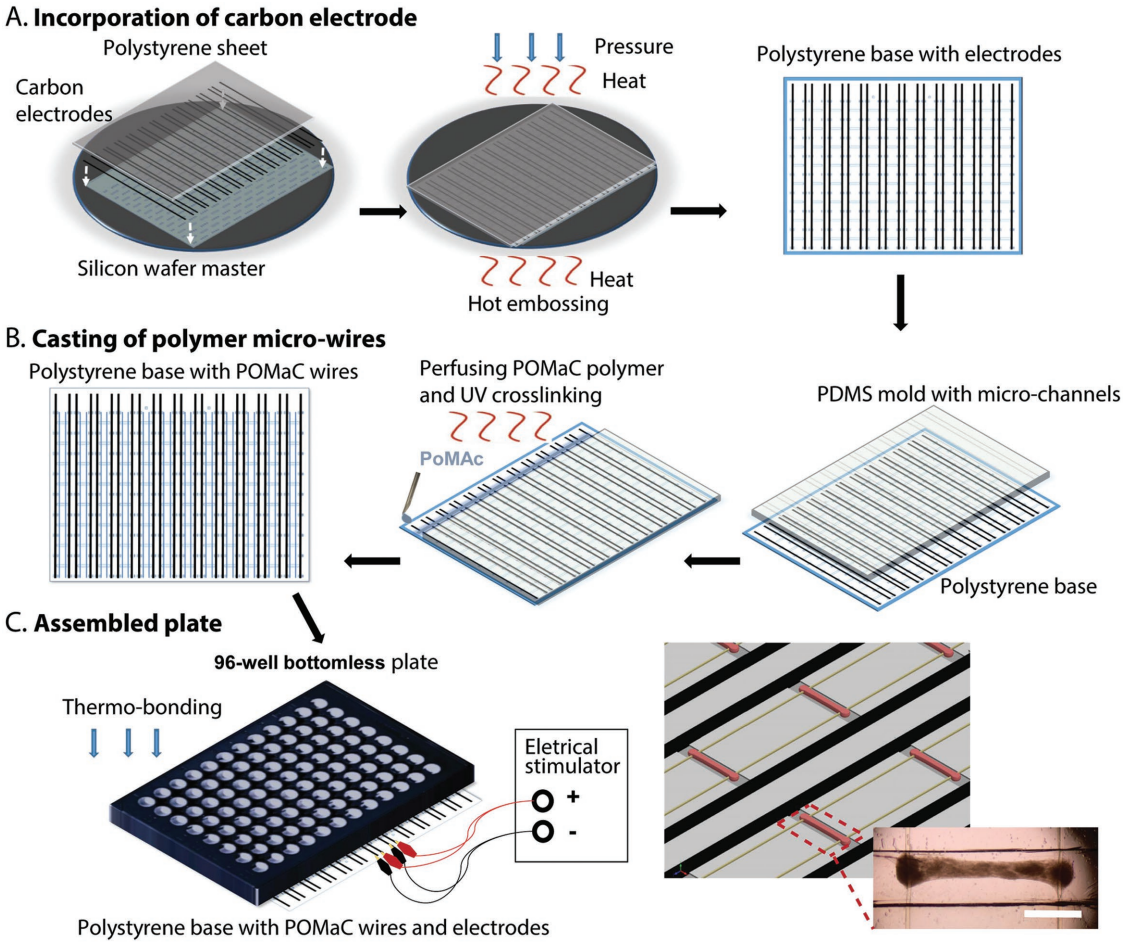

Figure 1. Overview schematics of the Biowire 96-well plate fabrication. A) Incorporation of carbon electrodes to Biowire plate base. B) Casting of polymer microwires to Biowire plate base. C) Assembled Biowire plate and representative image of a cardiac tissue cultured in the Biowire chamber and suspended across two polymer wires in parallel. Scale bar, 1 mm.

and bottomless 96-well plate are commercially available components. The polystyrene plate base was customized to match the 96-well plate format, with one microwell ($L \times W \times H$: $5 \times 1 \times 0.2$ mm) that aligns with the center of each bottomless well (Figure 1A). Human pluripotent stem cell derived cardiomyocytes (hCMs) and human cardiac fibroblasts (10:1 ratio) in a hydrogel matrix (3.0 mg mL^{-1} collagen and 15% (v/v) Matrigel) were cast in the microwells. To provide anchor points for tissue remodeling and compaction, two elastic microwires (diameter: 0.1 mm) positioned in parallel were cast across the microwell (Figure 1B). Over time, hCMs/fibroblasts/hydrogel mixture seeded in the microwells self-organized into a 3D tissue suspended and anchored across the two parallel wires (Figure 1C). Within one week, the tissues began to contract, bending the elastic polymer wires. Using calibration curves generated by a standard force sensor (MicroSquishier, CellScale) we were able to correlate the displacement of the polymer wires with the tissue contractile force.

Although the entire device fabrication process can take up to six days, most steps that involve manual operation are short and multiple plates can be produced in parallel (Figure S1A, Supporting Information). The fabrication of the polymer wires and the base plate are concurrent. For these components, an SU-8 master mold was designed and fabricated using standard soft-lithography techniques according to the specifications shown in Figure S1B,C in the Supporting Information. PDMS was then cast onto the SU-8 master to create a PDMS mold by crosslinking the PDMS at room temperature for 48 h. PDMS molds were then used to produce polymer wires, as well as to enable hot embossing of the polystyrene base plate. We chose to crosslink PDMS mold at room temperature rather than under heat to minimize the effect of thermal expansion. Thus, the resultant PDMS mold will retain the designed dimensions across a large surface area, such as the footprint of a 96-well plate. However, thermal expansion was still encountered during hot embossing of the base plate. Initially, we found that it was challenging to maintain the predefined plate dimensions without any shrinkage across this large footprint. Even a shrinkage of 0.1 mm across a length of 100 mm can result in significant misalignment between the wire and the microwells. Therefore, we empirically determined the degree of shrinkage after hot embossing, and readjusted the dimension of wire array to match the final dimensions of the plate base (Figure S1B, Supporting Information).

2.2. PDMS-Based Master Mold for Hot Embossing

To make the polystyrene base plate, the back of the base plate PDMS mold was bonded to a 6 in. silicon wafer with plasma bonding or corona etching methods. Following bonding to the silicon wafer, the mechanical properties of the PDMS master were further strengthened by exposing to 150 °C for 30 min. A polystyrene sheet was molded against the PDMS master in a hot embosser, which yielded a customized polystyrene plate base. The fabrication of the PDMS master for hot embossing is significantly cheaper than the conventional metal etching approach to create a master. Although PDMS is softer than metal, which might lead to feature distortion during the hot-embossing process, we found that this issue can be circumvented by using low compression force with high temperature during embossing. One important benefit of a PDMS over a metal-based master is its ability for temporary distortion, to allow the easy release of embossed polystyrene sheet from the master. This is a major challenge when a hard material (polystyrene) is embossed against another hard material (metal master) where microfeatures must strictly possess vertical walls to prevent interlocking of two hard materials.

The plate incorporates a pair of built-in carbon electrodes around every microwell to generate a local electrical field across each tissue. Pacing the cardiac tissue with external electrodes has been shown to both mature the tissue over time and standardize beating frequency to ensure consistency in drug testing.[6] For each column of wells, two long carbon electrodes were placed along the vertical well borders. Figure S1C in the Supporting Information shows the design of the base plate. The rectangular posts around the microwells were designed to hold the carbon electrodes to the PDMS master mold prior to hot embossing (**Figure 2**A). The carbon electrodes were embedded into the polystyrene sheet during hot embossing and were exposed on the plate surface and the side walls that make up the microwells (Figure 2B,C). These exposed surfaces were strategically positioned to be as close to the tissue as possible and were sufficient to generate an electrical field along the tissue length. With embedding of electrodes with a thickness of 400 μm into the polystyrene base, electrical current was able to pass through with minimal resistance. This is beneficial in contrast with other methods, including our initial trials with sputtering (e.g., sputtered gold electrodes) that resulted in a thin conductive surface with a thickness on the nanometer scale (Figure S2, Supporting Information). We found such conductive surfaces are difficult to coat uniformly across a large surface area, were easily damaged by scratching, resulted in high electrical resistance, and lacked long-term stability due to delamination (Figure S2, Supporting Information). The percentage of voltage drop across the embedded carbon electrodes, compared to the voltage applied from the source, was negligible and consistent across the well-plate. (Figure S3, Supporting Information).

2.3. Rapid Wire Casting on Microwells

The casting of soft elastic polymer microwires suspended across an array of microstructures in a scalable manner can be challenging. To avoid this, we developed a method of molding and crosslinking the polymer wires directly over the microwell structure on the polystyrene base. To do this, the PDMS mold of the wire array was caped on top of the base plate with the microchannels on the mold facing the plate (**Figure 3**A). Poly(octamethylene maleate (anhydride) citrate) (POMaC)[13] prepolymer, a citric acid based polyester that can be crosslinked with UV light or heat energy, was deposited at the channel inlet. The prepolymer solution was drawn into the microchannels via capillary action. Notably, the prepolymer solution continuously filled the channels over the microwells, even though the cross-section of microchannels were not fully closed (Figure 3B). Following full perfusion, the POMaC prepolymer was exposed

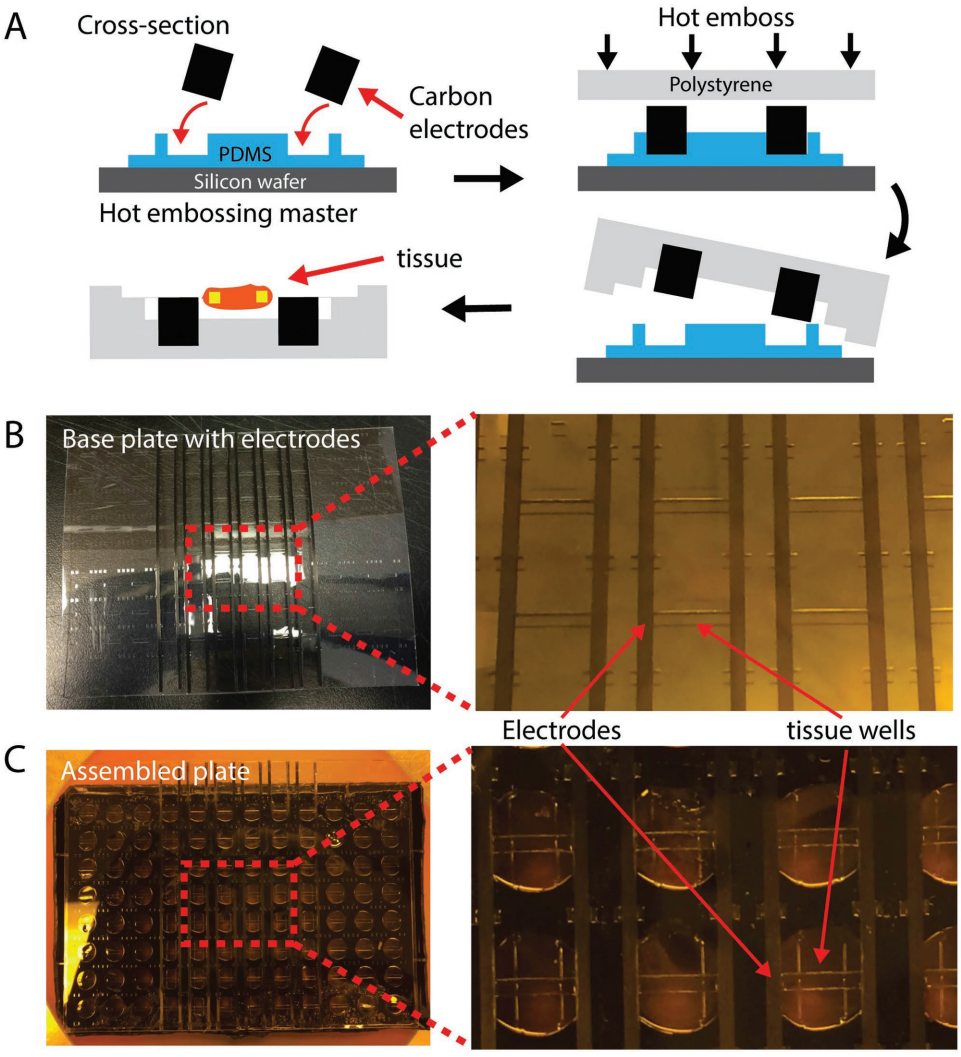

Figure 2. Biowire plate base hot embossing, assembly, and post-treatment. A) Illustration of hot-embossed polystyrene plate base embedded with carbon electrodes. B) Image of a polystyrene plate base embedded with carbon electrodes. The top surface of the carbon electrode is always exposed. C) Biowire plate completely assembled with both polymer wires and carbon electrodes viewed from the back side. Arrows indicate the location of carbon electrodes and tissue chambers.

to UV light to generate an array of crosslinked elastomeric wires, after which the PDMS mold was removed. To mitigate the effects of batch-to-batch variation of the bulk polymer solution to the mechanical stiffness of the UV-crosslinked polymer wires, the UV crosslinking energy was adjusted for each batch of polymers so that the Young's modulus (measured with a myograph as we described[14,15]) of the bulk polymer after crosslinking is 33 ± 3 kPa. UV-crosslinked POMaC wires consistently attached to the polystyrene base, resulting in multiple microwires cast across the entire plate, suspended across 96 microwells (Figure 3C). This method enabled installation of 24 wires suspended across 96 microwells in a single step. The plate base cast with microwires was then fully assembled with a heat bonding step in the hot embosser to fuse a bottomless 96-well plate onto the polystyrene plate base casted with polymer microwires. Then, the assembled plate went through several postprocessing steps including washing in distilled water overnight, air drying, packaging, and gamma-ray sterilization. The elasticity of the microwire can be further fine-tuned with additional heat crosslinking by baking the entire plate at 70 °C for several days. The plates were stored at 4 °C and protected from light prior to use to minimize unnecessary heat and light exposures prior to use.

2.4. Plate Characterization and Use

The cast polymer wires in the plate were used as both anchor points for tissues and force sensors to monitor change in contraction. To do so, the correlation between wire displacement and force generation was characterized. We used a commercially available microscale mechanical testing system, MicroSquisher (CellScale), to develop a force–displacement calibration curve (**Figure 4**A–D). The probe tip was customized with a curvature similar to the tissue attachment to polymer wires. With the probe tip moving against the polymer wire at

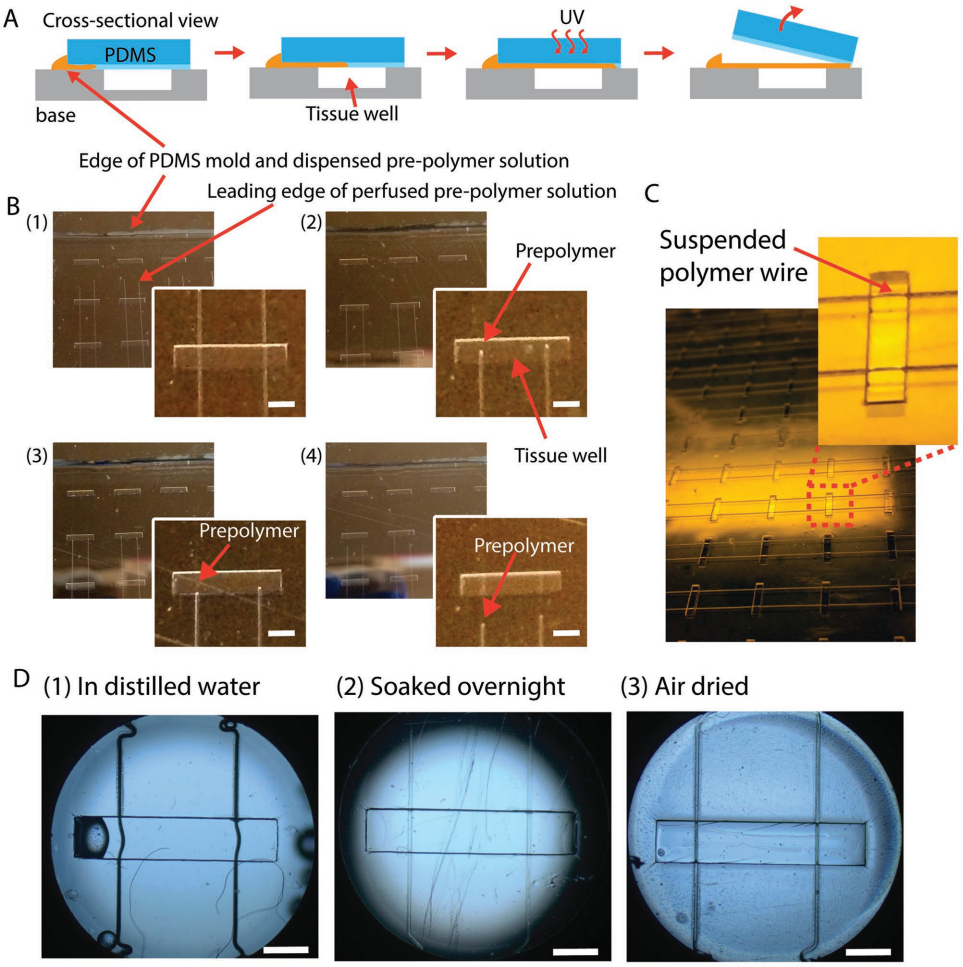

Figure 3. Rapid casting of suspended polymer wires in a 96-well plate format. A) Illustration of polymer injection molding, UV crosslinking, wire casting, and mold release. B) Images of polymer injection with capillary forces showing the polymer solution was able to perfuse across the suspended microchannel above the tissue chamber. C) Image of polymer wires successfully suspended across tissue chambers after mold removal. D) Images of the assembled Biowire plate soaked in distilled water 1) after 1 min, 2) after 24 h, and 3) after air-drying. Scale bar, 1 mm.

its center point, both force and displacement were recorded by MicroSquisher to develop force–displacement curves (Figure 4A, and Video S1, Supporting Information). The mechanical properties of the polymer wires can be further fine-tuned in postprocessing by heat crosslinking. After two, four, and six days of heat crosslinking, the force–displacement curves and fitted polynomial equations are shown in Figure 4B–D. The mechanical consistency of POMaC wires were demonstrated across the 96-well plate. There were no significant differences when the forces at 100 µm wire displacement were compared among the wells from different columns (Figure S4A, Supporting Information). The forces required to displace the wire for 50, 100, and 150 µm were also reproducible among all the wells (Figure S4B, Supporting Information). Furthermore, the tensile and relaxation curves of a representative polymer wire showed a minimal hysteresis (Figure S4C, Supporting Information). Microtissues cultured in each 96-well plate were able to grab the wires (**Figure 5**A). The cardiac tissues also displayed well-aligned sarcomere structures when stained for sarcomeric α-actinin (green) and F-actin (red) (Figure 5B). Since 96-well plates are a widely adopted tissue culture format, we demonstrated that the Biowire plate is also compatible with commercially available instruments, such as SpectraMax image cytometer for automatic imaging and analysis (Figure 5C).

2.5. Long-Term Tissue Culture and Drug Testing with Electrical Stimulation

To characterize the utility of the platform for in situ measurements (e.g., force–displacement) and to conduct proof-of-principle studies to demonstrate that the platform can support long-term cultures of cardiac tissues in a way similar to Biowire I,[6] we then tracked the functional responses of the cardiac tissues cultured on the platform under electrical stimulation and treatments with clinically relevant drugs. To generate cardiac tissues, human iPSC derived cardiomyocytes cocultured with human cardiac fibroblasts were seeded with hydrogel in the 96-well plate device. Tissue compaction in the first seven days was observed (**Figure 6**A,B), with dramatic change in the first two days followed by stabilization after day 3. Electrical field stimulation of cardiac tissues was initiated at day 7 and

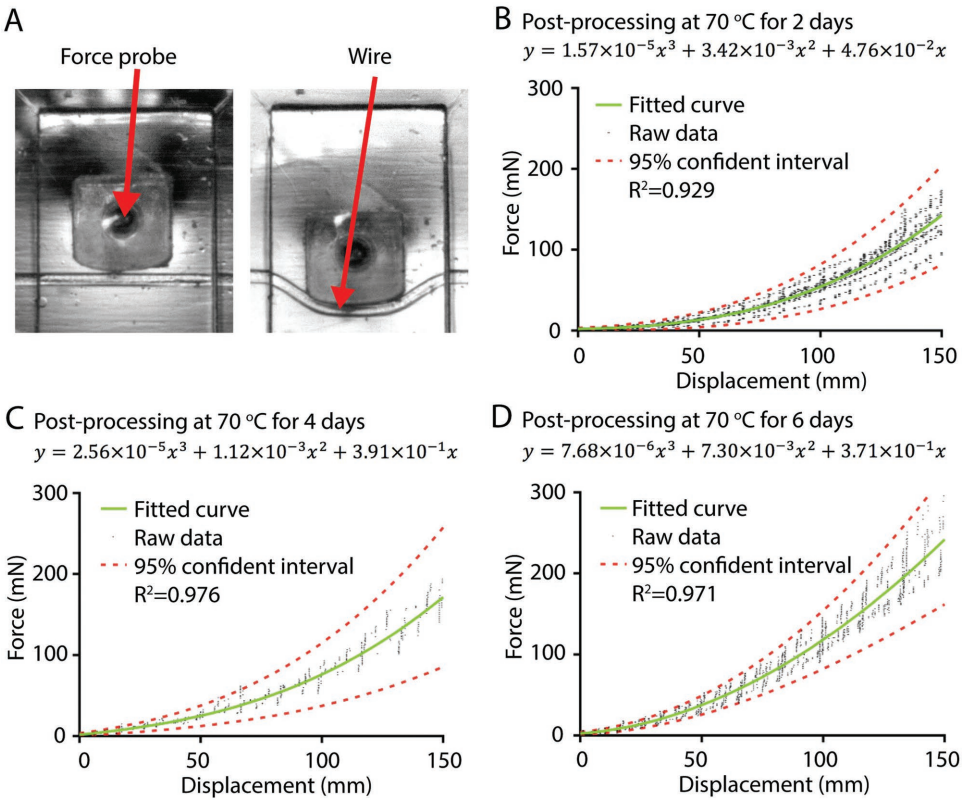

Figure 4. Characterization of polymer wires in the 96-well plate device. A) Images of a force probe used to deflect the polymer wire to correlate force and displacement. B–D) Force–displacement curves for the POMaC wires obtained after (B) two days ($n = 8$), (C) four days ($n = 3$), and (D) six days ($n = 7$) of postprocessing baking at 70 °C. The graphs show the raw data traces for individual force–displacement curves with 95% confidence intervals around the mean value, the polynomial equations and R^2 values of the fitted curves.

continued for the additional 12 days. During this period, the electrical functionality of the tissues was improved as observed through a significantly increased maximum capture rate (Figure 6C,D). The plate facilitated nondestructive evaluations of tissue contractile dynamics, which showed that passive tension, active force, time for contraction, and relaxation remained

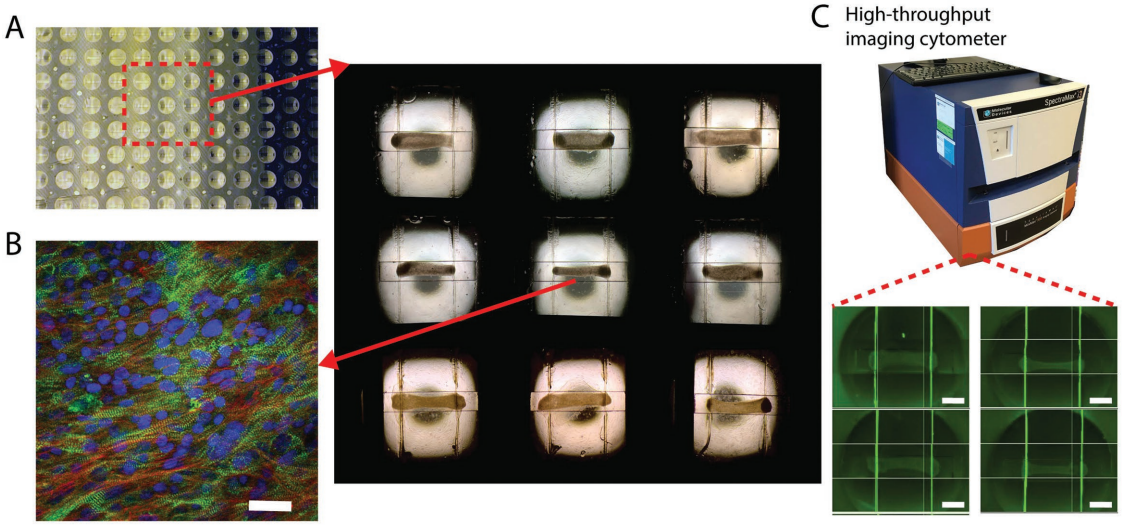

Figure 5. Characterization of cardiac tissue cultured in the 96-well plate device. A) Brightfield image of cardiac tissues cultured in Biowire II 96-well plates. The final image was stitched from multiple images. B) Fluorescent image of a cardiac tissue cultured in a 96-well plate device stained for sarcomeric-α-actinin (green) and F-actin (red). Scale bar, 30 µm. ($n = 3$) C). Fluorescent image of cardiac tissues imaged automatically in a SpectraMax image cytometer. The images clearly show the autofluorescent polymer wires in green, potentially enabling the tracking of wire displacement over time in high-throughput. Final image stitched from multiple images. ($n = 4$) Scale bar, 1 mm.

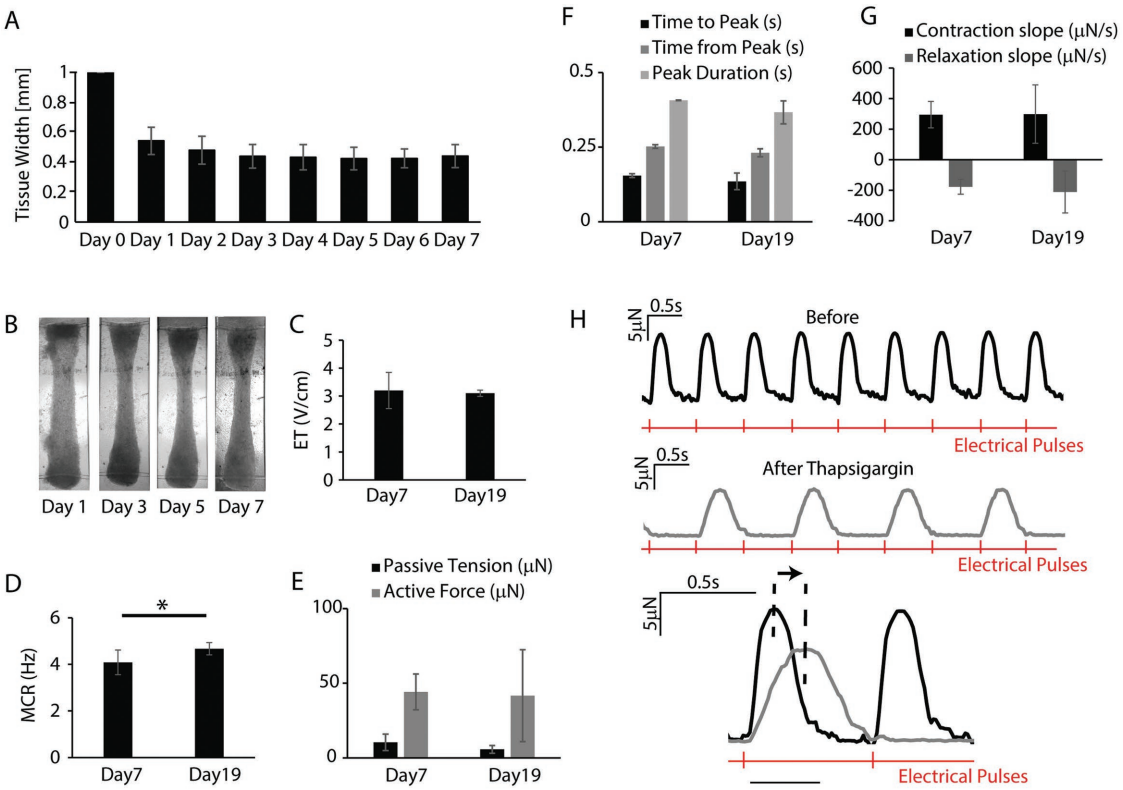

Figure 6. Functional assessment of human engineered cardiac tissues and their responses to thapsigargin after 12 days of electrical stimulation with built-in carbon electrodes. A) Tissue dimensions stabilized after seven days of self-organization observed through B) daily representative images ($n = 3$). Enhanced electrical properties were indicated by a C) decreasing trend of excitation threshold and D) significantly increased maximum capture rate (Student's t-test, $n = 6$) comparing day 7 (before electrical conditioning) and day 19 (end point). The 96-well plate device enables nondestructive force readouts and beating characterization of cultured tissues. Quantification of E) passive tension, active force, F) time of contraction, relaxation, and the total duration, G) contraction and relaxation slopes were compared at days 7 and 19 ($n = 3$). H) Representative traces showing the responses of cultured tissues to thapsigargin at the end point of electrical stimulation (day 19) ($n = 2$). Data are presented as mean ± standard deviation and differences between experimental groups were analyzed by Student's t-test. *$p < 0.05$ was considered significant for all the tests.

stable after 12 days of electrical stimulation (Figure 6E–G). Thapsigargin (50×10^{-6} M), an inhibitor of sarcoplasmic reticulum function in cardiomyocytes, was added in the presence of electrical pacing (1.5 Hz), resulting in a prolonged tissue contraction and relaxation time (Figure 6H). Furthermore, the frequency of tissue beating was decreased by half upon drug application despite the constant stimulation frequency (Figure 6H).

3. Discussion

In this study, we developed a new method to rapidly cast suspended elastic microstructures (e.g., wires) onto an array of microfabricated topographical features (e.g., microwells). Thermal bonding with a hot embosser allowed us to fuse multiple parts of the plate together and to embed both carbon electrodes and polymer wires into the platform to create a controlled micro-environment around the tissue. Tissue function and response can be manipulated with electrical stimulation and tracked with built-in force sensors. In this multiwell plate format, each tissue was independently cultured and analyzed. Although the entire manufacturing process requires six days from production to storage, the entire process is scalable as the production workload will not increase with increasing number of wells in the plate. This means the same process could be adapted to make 6-well, 24-well, 96-well, or even 386-well plates. Furthermore, multiple plates can be fabricated in parallel to achieve higher production throughputs, compatible with industrial manufacturing process. Up to 96 tissues can be cultured on a single plate; an experimentation throughput is significantly higher than in many conventional organ-on-a-chip platforms. Furthermore, the formation of a cardiac tissue takes as few as 100 000 cells. Currently, cell seeding is still a limiting step for high-throughput tissue production. However, enabled by the open well design, automatic cell dispensers[16] that are widely available in the pharmaceutical industry, could be used to scale up the cell-seeding and operation of this multiwell plate platform.

Material postprocessing after plate assembly also allowed adjustment to the deflection-force profiling in this system. By characterizing the mechanical properties of the elastic microwires, the functional readouts of tissue contractile dynamics can be deduced. The mechanical properties of the POMaC wire were reproducible among all the wells in the 96-well plate, which indicates the reliability of this casting method. Since the

polymer wires are always positioned at the identical height, the tissue height is always constant enabling easy monitoring, in contrast to postbased platforms,[9] where tissue vertical position is nonuniform. Nondestructive functional readouts are crucial for long term chronic drug studies. For our application, we demonstrated rapid casting of soft elastic microwires for the purpose of cardiac tissue culture. However, more complex suspended microstructures could be cast to enable the formation of more complex tissue structures with the same method. This platform also incorporates built-in electrodes that can stimulate tissues continuously for at least 12 days to assist in tissue maturation. The highly conductive carbon electrodes minimized the voltage drop from the voltage source to the electrodes, therefore facilitating a precise control of culture and testing environment. The presence of electrodes plays a crucial role in probing drug responses. For instance, when testing drugs in acute or chronic formats, chronotropic effects from the drugs can be isolated from inotropic effects by stimulating the tissue at a physiologically relevant frequency. With thapsigargin treatment, we showed slowed tissue contraction and relaxation, and a reduced frequency despite of the fixed pacing frequency. This implied the relaxation of the tissue was too slow to start the next depolarization until the relaxation of the previous contractile cycle is finished, thus, the frequency is reduced by half. Therefore, our platform was able to recapitulate the known in vivo effects of this compound, suggesting its applicability as a relevant in vitro screening platform.

4. Conclusions

Herein, we described a facile approach to manufacture an array of elastic microwires for scalable 3D cardiac tissue culture and contractile force readout in a 96-well plate format. This arrayed tissue culture plate can facilitate microscale tissue cultivation with a minimal number of cells, promote cardiomyocyte maturation with built-in carbon electrodes, as well as provide noninvasive functional assessments for cardiotoxicity prediction. Based on the ease and high throughput of fabrication, and the availability of high-fidelity cardiac tissue, the featured platform provides a valuable tool for assessing tissue responses of pharmacological compounds.

5. Experimental Section

POMaC Prepolymer Solution Preparation: POMaC[13] was used to prepare the built-in polymer sensors. POMaC was synthesized by first preparing a prepolymer gel through a polycondensation reaction. Citric acid (Caledon, A00019), maleic anhydride (Sigma, 63200), and 1,8-octanediol (Sigma, O3303) were combined in a triple necked 250 mL round bottom flask with an equimolar amount of carboxylic acid (citric acid + maleic anhydride) to alcohol (1,8-octanediol) functional groups and a 1:4 ratio of citric acid to maleic anhydride. The reaction solution was heated to generate a melt polymerization solution and carried out at 150 °C with stirring at 200 rpm for 5 h under nitrogen flow. The resultant gel was dissolved in 1,4-dioxane (Sigma, D201863) followed by a dropwise precipitation in deionized water to remove unreacted monomers or short chain oligomers. The aqueous phase was then decanted and undissolved prepolymer was collected and concentrated. Purified prepolymer was mixed with poly(ethylene glycol) dimethyl ether (PEGDM Mw ≈ 500) (Sigma, 445886) at 6:4 (w:w) ratio and 5 (w/w)% photo-initiator, 2-hydroxy-1-[4(hydroxyethoxy)phenyl]-2-methyl-1-propane (Sigma, 410896). The resulting solution was stored at 4 °C until use in sensor casting.

Fabrication of Base Plate with Built-In Carbon Electrodes: A repeated pattern consisting of rectangular microwells (5 × 1 mm, $L \times W$) and rectangle notches (1 × 0.5 mm, $L \times W$) was designed with AutoCAD. Spacing from adjacent microwells (in all directions) was 9 mm to achieve compatibility with conventional 96-well tissue culture plates. Using soft lithography, an SU-8 photoresist master mold was generated using a photomask derived from the computer model and used to produce a negative PDMS (Sylgard 184 silicone elastomer kit, Dow Corning, 01064291) master mold[14] with a feature height of 200 µm. Briefly, silicone elastomer base and the curing agents were vigorously mixed in the cup at 5:1 (w:w) ratio and the mixture was poured onto the SU-8 master mold to cure at room temperature. The PDMS master mold was then fixed to a silicon wafer by plasma bonding or corona etching. To embed the electrodes into the polystyrene base plate, carbon electrodes were first placed on the PDMS mold and fixed between the rectangle notches. Carbon electrodes were custom computer numerical controlled (CNC) machined at Ohio Carbon Blank. The electrodes were isostatically pressed carbon/graphite (Cat No. AR-14, Ohio Carbon Blank). Then a blank polystyrene sheet and a silicon wafer were placed on top and loaded into an EVG 520 Hot Embosser. The temperature and pressing force were gradually increased to 190 °C and 3000 N, with an internal pressure of 5×10^{-3} mbar. After temperature and pressure returned to ambient conditions, the resultant patterned polystyrene base embedded with carbon electrodes was released from the PDMS mold. The edges were trimmed and ready for use.

Fabrication of PDMS Mold and Wire Installation in Batch: To fabricate the POMaC wires, a PDMS mold with 24 microchannels (cross-section: 100 × 100 µm) positioned in parallel was fabricated from a SU-8 master mold, as previously described.[14] Silicone elastomer base and curing agent were vigorously mixed in the cup at 15:1 ratio and the 15 g of the mixture was poured onto the SU-8 master mold to cure at a room temperature. With edge trimming to vertically open the channel ends, the channel side of PDMS mold was cleaned with clear tape to remove dust particulate. The PDMS mold was then gently pressed on top of the embossed polystyrene sheet with adjustment of channel position and orientation and position to align the polymer wire location with the microwells. POMaC prepolymer solution was dispensed to the top edge of the PDMS mold with a syringe, and the prepolymer was perfused by capillary action in the dark for 48 h at room temperature. Following perfusion, the polymer was crosslinked under UV light (1500 mJ cm^{-2}) to generate an elastomeric material network. The excess nonperfused POMaC polymer was removed and the PDMS mold was slowly peeled away from the plate base, leaving behind the polymer wires which remain adhered to the polystyrene sheet.

Thermal Bonding of Base to a Bottomless 96-Well Plate: A bottomless 96-well plate was placed, base up, on a flat surface and a base plate equipped with wires and electrodes was placed against it, aligned to center the polymer wire pairs in individual wells. A drop of acetone was applied at the corners of the plate between the base and the plate to temporarily bond the plastic layers, then the combination was fully bonded by hot embossing. The base face was gradually heated to 184 °C with a pressing force of 700 N, and an internal pressure of 5×10^{-3} mbar with maintenance of the top heating surface at 96 °C.

Postassembly Processing: Following the embossing process, wells of bonded plates were filled with distilled water and incubated overnight (37 °C, 5% CO_2). Water was then removed and the plate was air dried under sterile conditions. The plate was then baked (70 °C) for six days and subjected to gamma ray sterilization. After sterilization, the plate was stored at 4 °C shielded from light.

Plate Characterization: To measure the bulk polymer Young's modulus, a myograph machine (Kent Scientific), composed of a mechanical stretcher and a force transducer, was used to stretch strips of POMaC polymers (0.3 × 1 × 10 mm) crosslinked with UV light (1500 mJ cm^{-2}) in PBS solution. The slope of the resulting stress–strain curve was used to calculate the Young's modulus. Polymer wire force/displacement

curves in the wells were characterized using a commercially available micromechanical tester, MicroSquisher (CellScale) (Video S1, Supporting Information). Testing probes (diameter = 0.1524 mm) were modified with customized tips (half ellipse, 4:1 diameter ratio with long diameter of 0.5, 0.7, and 0.8 mm) fabricated from an SU-8 master by soft lithography and attached to the provided tungsten probe using an adhesive (T-GSG-01 Titan Gel). Polymer wires were soaked in medium for seven days prior to testing. Testing tips were centered in the microwell, then polymer wires were displaced at the center using the probe tips moving perpendicular to the long axis of the wire, with recording of the corresponding force output ($n \geq 12$). The experimental data for each custom tip were fit to a third-degree polynomial equation, generating a standard force curve for each custom probe. For consistency across the plate, measured forces at 100 µm displacement were compared among right wires in each well. The two outermost columns were omitted from the measurements on purpose, as it was found that the pressure at the edges created nonuniformities in the two outermost columns.

Voltage Drop along the Electrode: After the plate assembly, carbon electrodes along a column were connected to a voltage source (9 V battery). A handheld multiscope (Extech, 381275) was used to measure the voltage differences across each pair of carbon electrodes in different wells ($n = 3$ wells per row). Voltage drop was calculated using the differences in the voltage between the carbon electrodes and the voltage source divided by the voltage from the voltage source.

Hydrogel Preparation: Collagen hydrogel (500 µL) was prepared by combining high concentration rat tail collagen (153 µL at 9.82 mg mL^{-1}, Corning) with 15% (v/v) Matrigel (75 µL, BD Biosciences), $NaHCO_3$ (50 µL at 2.3 mM, Sigma), NaOH (5 µL at 10 mM, Sigma), deionized sterile H_2O (167 µL) and 1× M199 (50 µL, Sigma) to result in a final collagen concentration of 3.0 mg mL^{-1}.

Cardiomyocyte Preparation and Generation of Engineered Cardiac Tissues: Predominantly ventricular cardiomyocytes (CMs) were derived from the hiPSC line BJ1D, using monolayer differentiation protocols as previously described.[17,18] At day 21 of differentiation, cardiomyocytes were disassociated into single cells with previously established methods.[18] Briefly, 1 mg mL^{-1} of collagenase type II (Worthington, LS004205) in Hank's Balanced Salt Solution was added to the monolayer cardiomyocyte cultures and incubated overnight at room temperature. The disassociated cells were mixed with cardiac fibroblasts (Lonza, NHCF-V) in a 10:1 cell number ratio. The mixed cells were pelleted and remixed in collagen hydrogel at 5.5×10^7 cells mL^{-1}. The cell-gel mixture was seeded at 2 µL per microwell. A droplet of media was placed on the wall of the well to keep the moisture until gelation was complete. The plate was incubated at 37 °C and 5% CO_2 for 10 min followed by media addition. After seeding (day 0), the tissues were cultured for seven days to allow remodeling around the POMaC wires. Bright field images of the tissues were taken daily to monitor tissue morphology. By day 7, the tissues synchronously contracted and deflected the POMaC wire with each contraction.

Imaging Tissue Morphology in Batch: SpectraMax MiniMax 300 Imaging Cytometer was used to image tissues in the well plate to monitor the daily morphology changes of tissues. Nine pictures were taken in each well of the 96-well plate and automatically stitched together to show the entire view of the well.

Contractile Analysis via 4′,6-Diamidino-2-Phenylindole (DAPI) Channel Imaging: Spontaneous and paced (1 Hz) contraction was imaged using bright field microscopy (4× objective). The blue channel (10× objective; $\lambda_{ex} = 350$ nm, $\lambda_{em} = 470$ nm; 100 frames s^{-1}, 5 ms exposure) was used to record and analyze tissue contractile behavior, and data was output using custom MATLAB code to track wire displacement. Average tissue width and width of the tissue (Tw), attachment site to the polymer sensor were measured using bright field images at the relaxed state. Passive displacement of polymer sensors was assessed in blue channel. Total deflection and passive deflection of polymer sensors (µm) were converted to force (µN) using calibration curves that were generated as described in the plate characterization section. The final readouts for the total and passive forces were interpolated according to the Tw and custom tip sizes. The active forces were the difference between total and passive force. The custom MATLAB code was used to calculate the passive force, active force, contraction, and relaxation duration.

Immunostaining and Confocal Microscopy: Tissues were fixed with 4% paraformaldehyde, permeabilized with 0.2% Tween20, and blocked with 10% fetal bovine serum. Immunostaining was performed using the following antibodies: mouse anti-α-actinin (Abcam; 1:200) and the donkey anti-mouse-Alexa Fluor 488 (Abcam; 1:400). Phalloidin-Alexa Fluor 660 (Invitrogen; 1:200) was used to stain F-actin fibers. Confocal microscopy images were obtained using an Olympus FluoView 1000 laser scanning confocal microscope (Olympus Corporation).

Tissue Maintenance and Drug Testing with Electrical Stimulation: Each well of 96-well plate contained 300 µL of culture medium, which was changed every 24 h. With built-in force sensor and electrodes, tissues were able to be assessed in situ in terms of their contractile dynamics and drug responses. Before testing, a bright field video of tissue was taken to obtain necessary measurements for force calculation. During testing, pacing voltage was increased to 110% of excitation threshold. One polymer wire (blue channel, 10× magnification) was imaged consistently for comparison. Once baseline video was taken, 0.3 µL of thapsigargin (50×10^{-3} M in DMSO) was added into the well with gel-loading pipette tip. After 15 min, video was taken again after thapsigargin was in effect. The videos were analyzed using the custom MATLAB software.

Statistical Analysis: Statistical analysis was performed using Sigma Plot 12.0 or Prism 6.0. Differences between experimental groups were analyzed by Student's *t*-test or one-way ANOVA. Normality test (Shapiro–Wilk) and pairwise multiple comparison procedures (Tukey or Holm–Sidak method) were used for one-way ANOVA. $p < 0.05$ was considered significant for all statistical tests. All data were shown as mean ± standard deviation. Sample size (n) for each statistical analysis was stated in the Figure captions.

Supporting Information

Supporting Information is available from the Wiley Online Library or from the author.

Acknowledgements

This work was made possible by the National Sciences and Engineering Research Council of Canada (NSERC) Postgraduate Scholarships-Doctoral, Ted Rogers Education fund and TOeP NSERC CREATE scholarship awarded to Y.Z., the NSERC Steacie Fellowship to M.R., and the CIHR Banting Postdoctoral Fellowship to B.Z. This work was funded by NSERC-CIHR Collaborative Health Research Grant (CHRP 493737-16), National Institutes of Health Grant (2R01 HL076485), the Canadian Institutes of Health Research (CIHR) Operating Grants (MOP-126027 and MOP-137107), and NSERC Discovery Grant (RGPIN-2015-05952) to M.R. Y.Z. and E.Y.W. performed the experiments, analyzed the results, and prepared the manuscript. L.H.D. synthesized the polymer and performed the mechanical testing. Y.L. performed mechanical testing in different wells. K.Y. provided the carbon electrodes and offered guidance on the device design. G.V.N. edited the manuscript. M.R. envisioned the concept, supervised the work, and edited the manuscript. B.Z. developed the technology, analyzed the results, supervised the work, and prepared the manuscript.

Conflict of Interest

Y.Z., B.Z., G.V.N., and M.R. are among co-founders of TARA Biosystems and they hold equity in this company.

Keywords

cardiac tissue engineering, drug testing, organ-on-a-chip, platforms, polymer processing

Received: September 21, 2018
Revised: November 12, 2018
Published online:

[1] P. Liang, F. Lan, A. S. Lee, T. Gong, V. Sanchez-Freire, Y. Wang, S. Diecke, K. Sallam, J. W. Knowles, P. J. Wang, P. K. Nguyen, D. M. Bers, R. C. Robbins, J. C. Wu, *Circulation* **2013**, *127*, 1677.
[2] Y. Zhao, A. Korolj, N. Feric, M. Radisic, *Expert Opin. Drug Saf.* **2016**, *15*, 1455.
[3] S. Morgan, P. Grootendorst, J. Lexchin, C. Cunningham, D. Greyson, *Health Policy* **2011**, *100*, 4.
[4] G. Gintant, P. T. Sager, N. Stockbridge, *Nat. Rev. Drug Discovery* **2016**, *15*, 457.
[5] M. Tiburcy, J. E. Hudson, P. Balfanz, S. Schlick, T. Meyer, M. L. Chang Liao, E. Levent, F. Raad, S. Zeidler, E. Wingender, J. Riegler, M. Wang, J. D. Gold, I. Kehat, E. Wettwer, U. Ravens, P. Dierickx, L. W. van Laake, M. J. Goumans, S. Khadjeh, K. Toischer, G. Hasenfuss, L. A. Couture, A. Unger, W. A. Linke, T. Araki, B. Neel, G. Keller, L. Gepstein, J. C. Wu, W. H. Zimmermann, *Circulation* **2017**, *135*, 1832.
[6] S. S. Nunes, J. W. Miklas, J. Liu, R. Aschar-Sobbi, Y. Xiao, B. Zhang, J. Jiang, S. Massé, M. Gagliardi, A. Hsieh, N. Thavandiran, M. A. Laflamme, K. Nanthakumar, G. J. Gross, P. H. Backx, G. Keller, M. Radisic, *Nat. Methods* **2013**, *10*, 781.
[7] J. Shim, A. Grosberg, J. C. Nawroth, K. K. Parker, K. Bertoldi, *J. Biomech.* **2012**, *45*, 832.
[8] J. U. Lind, T. A. Busbee, A. D. Valentine, F. S. Pasqualini, H. Yuan, M. Yadid, S. J. Park, A. Kotikian, A. P. Nesmith, P. H. Campbell, J. J. Vlassak, J. A. Lewis, K. K. Parker, *Nat. Mater.* **2017**, *16*, 303.
[9] S. Schaaf, A. Shibamiya, M. Mewe, A. Eder, A. Stöhr, M. N. Hirt, T. Rau, W. H. Zimmermann, L. Conradi, T. Eschenhagen, A. Hansen, *PLoS One* **2011**, *6*, e26397.
[10] T. Boudou, W. R. Legant, A. Mu, M. A. Borochin, N. Thavandiran, M. Radisic, P. W. Zandstra, J. A. Epstein, K. B. Margulies, C. S. Chen, *Tissue Eng., Part A* **2012**, *18*, 910.
[11] M. W. Toepke, D. J. Beebe, *Lab Chip* **2006**, *6*, 1484.
[12] E. Berthier, E. W. Young, D. Beebe, *Lab Chip* **2012**, *12*, 1224.
[13] R. T. Tran, P. Thevenot, D. Gyawali, J. C. Chiao, L. Tang, J. Yang, *Soft Matter* **2010**, *6*, 2449.
[14] B. Zhang, M. Montgomery, M. D. Chamberlain, S. Ogawa, A. Korolj, A. Pahnke, L. A. Wells, S. Massé, J. Kim, L. Reis, A. Momen, S. S. Nunes, A. R. Wheeler, K. Nanthakumar, G. Keller, M. V. Sefton, M. Radisic, *Nat. Mater.* **2016**, *15*, 669.
[15] B. Zhang, B. F. L. Lai, R. Xie, L. Davenport Huyer, M. Montgomery, M. Radisic, *Nat. Protoc.* **2018**, *13*, 1793.
[16] S. Suomalainen, V. Kytöniemi, M. Mehto, *Reproducible Dispensing of Live Cells with the Thermo Scientific Multidrop Combi Reagent Dispenser*, Thermal Fisher Scientific, Vantaa, Finland **2009**.
[17] X. Lian, J. Zhang, S. M. Azarin, K. Zhu, L. B. Hazeltine, X. Bao, C. Hsiao, T. J. Kamp, S. P. Palecek, *Nat. Protoc.* **2013**, *8*, 162.
[18] L. Yang, M. H. Soonpaa, E. D. Adler, T. K. Roepke, S. J. Kattman, M. Kennedy, E. Henckaerts, K. Bonham, G. W. Abbott, R. M. Linden, L. J. Field, G. M. Keller, *Nature* **2008**, *453*, 524.